Journal of
Synchrotron
Radiation

ISSN 0909-0495

Received 28 December 2012
Accepted 14 July 2013

Local study of fissure caries by Fourier transform infrared microscopy and X-ray diffraction using synchrotron radiation

Pavel Seredin,[a]* Vladimir Kashkarov,[a] Anatoliy Lukin,[a] Yury Ippolitov,[b] Robert Julian[c] and Stephen Doyle[d]

[a]Solid State Physics and Nanostructures, Voronezh State University, Universitetskaya 1, Voronezh 394006, Russian Federation, [b]Voronezh State Medical Academy, Studencheskaya 10, Voronezh 394000, Russian Federation, [c]Synchrotron Radiation Center, 3731 Schneider Drive, Stoughton, WI 53589-3097, USA, and [d]Synchrotron Light Source ANKA, Hermann-von-Helmholtz-Platz 1, D-76344 Eggenstein-Leopoldshafen, Germany. E-mail: paul@phys.vsu.ru

Investigations of intact dental enamel as well as carious-affected human dental enamel were performed using infrared spectromicroscopy and X-ray diffraction applying synchrotron radiation. Caries of enamel was shown to be characterized by an increase in the number of deformation and valence vibrations for N—C—O, N—H and C═O bonds, a decrease of the crystallinity index, and by the absence of the preferable orientation of hydroxyapatite crystals within the affected enamel. This indicates the presence of destructive processes in the organic matrix of hard tooth tissues.

Keywords: human dental enamel; caries; X-ray diffraction; FTIR.

1. Introduction

Biological composites are currently of great interest, with many research groups involved in studying their properties, structure and functioning, attracting all kinds of modern methods of physical and chemical analysis of materials (Dunlop & Fratzl, 2010; Maertena *et al.*, 2013). Characteristic features of biological composites are as follows. On the one hand their number are small, but on the other hand they are characterized by versatility owing to a complicated structural hierarchy. Based on analysis of the literature it can be argued that enamel and dentin of human teeth are a good focus for research into biological composites. This is not surprising, given that dental caries is a major problem in modern dentistry and one of the main research fields of the science. According to many researchers, resistance to dental caries is related to the structure and properties of the hard tissues of the tooth.

Dental enamel is known to be the hardest human tissue. This allows it to withstand the impact of large mechanical loads while the tooth is performing its functions. It is well known that enamel consists of more than 90% of mineral compounds {mainly hydroxyapatite (HAP) [$Ca_{10}(PO_4)_6(OH)_2$], fluorapatite [$Ca_{10}(PO_4)_6F_2$] and carbonated apatite} and 1.2% of organic compounds, which refers to the bound water in crystals and organic components as well as free water (Bykov, 1998).

Data on the organic compounds contained in mature enamel are rather provisional. Jenkins (1978) presented the following numerical data on the content of organic compounds in the enamel of pre-molars and molars (% of dry solid matter): insoluble proteins, 0.3–0.4%; soluble proteins, 0.05%; fats, 0.6%; citrates, 0.1%. The most widespread proteins, about 90% of all the organic fraction, are hydrophobic proteins (amelogenins), enriched with amino acids and detected mainly in immature enamel, characterized by a high concentration of proline, glutamic acid, leucine and histidine; 10% are acidic proteins, *i.e.* enamelins, determined in completely mature enamel, arranged in the interprism substance with a high molecular mass and characterized by a high concentration of aspartic and glutamic acid, serine and glycine (Goldberg *et al.*, 1995).

Hard dental enamel is known to be in a state of permanent demineralization and remineralization; if the first kind of processes dominate over the second, caries may appear. The development of the caries process is accompanied by the formation of several different areas in the enamel: the translucent zone, dark zone, caries core and superficial zone. For different stages of the development of the caries process, especially for pigmented spots, the content of protein within the lesion shows a threefold or fourfold increase and this spot cannot transform into a carious cavity for several years; however, a considerable decrease in calcium and phosphorus is observed in this area, which is called demineralization. Prior to the appearance of the cavity within the hard dental tissue, the development of the caries process is reversible and the structure of enamel can be recovered. It is probable that protein plays an important role in the stabilization process and the reversibility of the process of focal de-

mineralization in hard dental tissues (Tiznado-Orozco *et al.*, 2009).

Organic matrix bound to crystals and providing their growth and orientation during formation of the enamel is almost completely lost during maturation of dental enamel. It is preserved in the form of a fine three-dimensional protein grid whose threads are located between the prisms. Recent investigations of the organic matrix of enamel provided new data on its nature and function. It was confirmed that its most important role is the stabilization of the buffer system providing the presence of free calcium ions in this system (Yamakoshi *et al.*, 2001). It should be noted that organic components of the enamel matrix have so far been studied to a lesser extent than its mineral phase. Calcium-binding protein that is capable of depositing in the neutral medium in the presence of calcium ions is considered as the functional elementary block of the organic matrix in the enamel. Calcium-binding protein of the enamel and acid-insoluble protein both determine the orientation of the crystals in enamel prisms and its structure. The significance of protein in enamel has not yet been studied and many consider that it plays only a passive role in enamel formation. However, there is a view that resistance to caries for the enamel depends not only on the content of inorganic components but also on the amount of protein. A 'protein grid' surrounding apatites of enamel prevents acid from contacting the apatite and also dampens its effect. Thus, understanding the processes taking place in enamel, both in its normal state as well as under pathological conditions, is largely dependent on knowledge of its constituents as well as on the connection between organic matrix and inorganic substance.

A number of investigations of human teeth have been performed previously, including studies with synchrotron radiation. Yagi *et al.* (2010) studied the early caries lesion in bovine tooth enamel using two different X-ray diffraction systems at the third-generation synchrotron radiation facility SPring-8 in Japan. The simultaneous small- and wide-angle measurement with a microbeam is a powerful tool for elucidating the mechanisms of demineralization and remineralization in early caries lesions.

The usefulness of integrated Fourier-transform infrared microscopy and X-ray diffraction studies in the evaluation of carbonated hydroxyapatite powders has been confirmed in work by Ślósarczyka *et al.* (2005).

As was shown by He *et al.* (2007), microstructural studies of hard dental tissue can be performed using Raman microspectroscopy. It was concluded that microspectroscopy provides a cutting-edge, high-resolution and non-destructive method for exploring the role of microstructure on the residual stress distribution within natural biocomposites.

However, in the main, hard dental tissue has been studied predominantly in its powder-like form (Tiznado-Orozco *et al.*, 2009; Low, 2004; Fried *et al.*, 2003), which is convenient for investigations using powder diffraction techniques, but is not ideal in this case.

Studies of the structure and chemical composition of intact and caries-affected dental enamel will give a more profound understanding of the original changes in hard dental tissues. Since the surface of the enamel at the initial stages of the caries process is relatively small, the most convenient and useful method to carry out this kind of study will be local diffraction of X-rays which provides valuable and detailed data on the mineral content of intact caries-affected teeth. As for the study of organic substances of enamel, it seems reasonable to apply IR Fourier spectromicroscopy, which allows the presence of organic (protein) components in the enamel to be revealed.

2. Objects and methods of investigations

A sample of a tooth with a caries lesion extracted from a patient with a case of severe paradontosis, according to orthodontic indications, was prepared as follows. First, the tooth was washed in flowing water, removing dental deposits, and then the surface was dried with filter paper. Next, using a specialized device with a diamond disc under water cooling, the tooth was sawed and as a result a plate of thickness up to 1 mm was obtained. The prepared slice was stuck onto a glass plate of thickness 2 mm using acrylic glue and was then ground and further polished with diamond paste. Fig. 1(*a*) shows a photograph of the analyzed sample.

At first, investigations were made at the Infrared Spectromicroscopy beamline of the SRC Aladdin synchrotron, University of Madison, USA, operating in the range 720–4000 cm^{-1}, using a Thermo Fisher Scientific Fourier spectrometer aligned with an IR microscope. The spot size was 25 mm $\times$ 12 mm (horizontal $\times$ vertical).

The area of the analyzed sample surface during a survey of IR spectra using a microscope was 20 µm $\times$ 20 µm. A study of the microstructure of the dental tissue by X-ray diffraction was performed at the ANKA-PDIFF beamline of the ANKA synchrotron, Karlsruhe, Germany. The radiation source was a 1.5 T swivel magnet arranged in the synchrotron ring (E_c = 6 keV). Monochromatic emission corresponding to Cu $K\alpha_1$ radiation with a wavelength of λ = 1.54032 Å was used in the experiments. Flux at the sample position was $\sim 2 \times 10^{10}$ photons s^{-1} mm^{-2} at 10 keV, based on 100 mA beam current and 0.1% bandwidth. The beam size at the sample was $\sim$0.5 mm (H) $\times$ 0.5 mm (V) (focused). In this case the analyzed area was 100 µm $\times$ 100 µm.

The points 1 and 2 shown in Fig. 1(*a*) were used for obtaining IR reflection spectra, while the points 3–5 in the carious canal shown in Fig. 1(*b*) were used for the local diffraction study.

3. IR spectromicroscopy

Application of IR microscopes operating in reflection mode as well as the high intensity of synchrotron radiation as a source of IR emission have allowed a rather successful analysis of the state of dental tissue by obtaining information from a small part of the polished surface (Fried *et al.*, 2003), which is in fact an even flat surface. Using Kramers–Kronig relations, we have recalculated IR-reflection spectra obtained in experiments

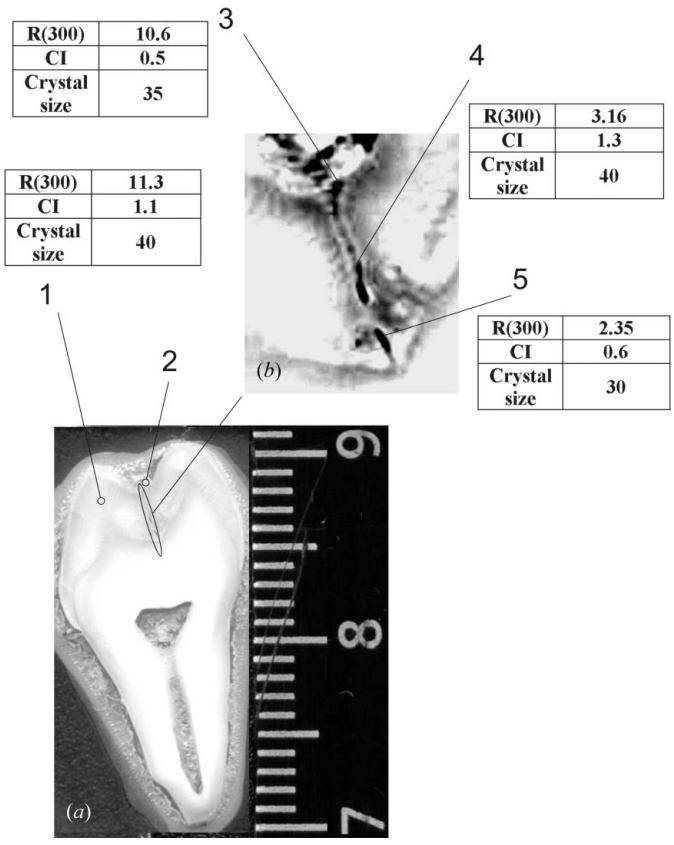

Figure 1
Frontal slice of the tooth where the investigated areas are indicated (right-hand scale in centimeters). (*a*) Full view of the tooth. (*b*) Fissure carious canal. Points 1–5 show the locations used for the study. The tabulated data show local diffraction analysis for points 1, 3, 4 and 5.

involving IR-absorption spectra since, in a number of works dealing with the analysis of IR spectra for dental enamel, IR-absorption spectra are usually presented (Karlinsey *et al.*, 2009; Krutchkoff & Rowe, 2009; Rey *et al.*, 2007). The spectral range from 2000 to 900 cm^{-1} was selected for the detailed analysis since only in this region can the main features determining the nature of dental enamel be observed. The results obtained are presented in Fig. 2.

As can be seen from this figure, IR-absorption spectra obtained from the investigated sample involve absorption bands characteristic of the dental enamel. The absorption spectrum obtained from the healthy (intact) enamel (1) differs considerably from that of the enamel affected by caries (2). In this spectral range the main absorption band related to the stretching vibrations $\nu(PO_4^{3-})$ in the spectrum (1) has its peak at 1035 cm^{-1}; it is rather narrow and has a weakly expressed 'shoulder' on the short-wavelength side. Two weak peaks beside this band can be quite easily seen at 1415 cm^{-1} and at 1450 cm^{-1} corresponding to the plane asymmetrical deformational vibrations $\delta_{AS}(CH_3)$. The bands of secondary amides, *i.e.* Amide I [ν(C═O), 1661.7–1664.2 cm^{-1}], Amide II [δ(C—N), 1555.8 cm^{-1}] (mixed stretching-deformational vibrations of N—H and C—N bonds) and Amide III [δ(NH), 1240.4 cm^{-1}], can be observed in the spectra of enamel

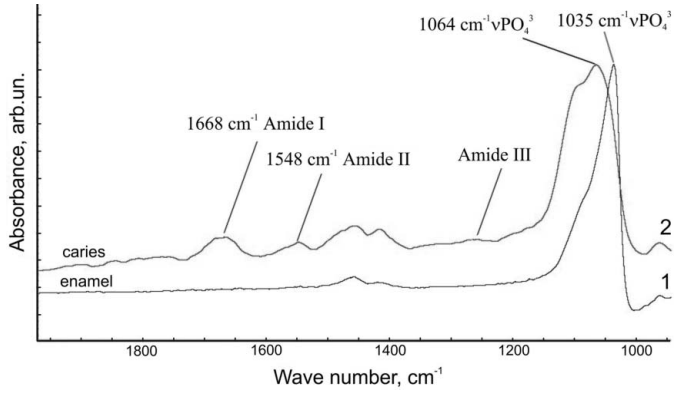

Figure 2
IR-absorption spectra. 1, intact enamel. 2, carious enamel.

affected by caries in addition to the bands related to inorganic constituents of the tooth. Since the observed absorption bands are connected to the presence of amino acids in the dental tissue, and the chains of these acids form protein, the value of their integral intensity makes it possible to form a conclusion on the protein concentration. A quantitative characteristic of the relative concentration for the protein component in the dental tissue can be the ratio of the integral intensity of Amide I, Amide II and Amide III absorption bands to the value of the integral intensity of the $\nu(PO_4^{3-})$ band, that characterizes the mineral (inorganic) component of the dental tissue. Calculations of this ratio were made with the use of the spectral software system *OMNIC*. The obtained data are presented for clarity in the form of histograms in Figs. 3(*a*) and 3(*b*).

Comparing the results of experimental investigations, a good agreement in the positions of the absorption peaks was found. This suggests that the results obtained are correct and certain observations can be made. For example, absorption bands related to the protein component (Amide I, Amide II) in all of the spectra are considerably smaller than those related to the mineral (inorganic) component. This can be clearly observed in the spectra as well as in the histograms. At the same time, the areas of enamel affected by caries or those arranged in their vicinity are characterized by the highest content of organic component, and the ratio of the component related to Amide I to that related to Amide II is approximately 2:1.

4. X-ray diffraction

The results of X-ray local diffraction for the investigated samples obtained in the range of angles of the most intensive lines in the spectra of synthesized microcrystalline bioactive hydroxyapatite (1), intact enamel (2), and three points of caries proliferation with an increase in depth, *i.e.* the beginning (3), center (4) and bottom of the fissure (5), are presented in Fig. 4.

The obtained experimental data suggest that Miller indices for the investigated materials correspond to synthetic calcium phosphate hydroxide (hydroxylapatite) $Ca_{9.868}(PO_4)_{5.586}$

Table 1
Results of X-ray diffraction analysis.

		Cell parameter		Texture index			
		a (Å ± 0.01 Å)	*c* (Å ± 0.01 Å)	*R*(300)	*R*(112)	Crystallinity index	HAP crystal size (nm ± 5 nm)
Synthesized bio HAP (Goloshchapov *et al.*, 2013)		9.40	6.87	–	–	–	40
Sound enamel (point 1, Fig. 1*a*)		9.44	6.88	11.3	2.1	1.1	40
Carious-affected enamel (Fig. 1*b*)	Point 3	9.44 (5)	6.88	10.6	4.7	0.5	35
	Point 4			3.16	2.6	1.3	40
	Point 5			2.35	2.9	0.6	30

$(OH)_{4.006}$, HAP. No additional phases on the basis of calcium are present in the samples.

Using the Rietveld method, we calculated parameters of the crystalline lattice for the analyzed areas of the tooth. The data are presented in Table 1.

As can be seen from Fig. 4, hydroxyapatite crystallites in the different analyzed regions of the human dental enamel are characterized by a clearly defined preferable orientation that can be observed by the change of intensity for the three strongest lines, (211), (300), (112), in the X-ray diffraction patterns of the samples.

In order to make some quantitative estimations of the degree of texture, one can use a value called the texture index, *R*, of a sample which can be determined by the ratio of intensities of the strongest lines, *I*(211)/*I*(300) and *I*(211)/*I*(112) (Low, 2004). For the reference sample of hydroxyapatite in powder form the ratio of intensities for the strongest lines in the diffraction spectrum are *I*(211)/*I*(300) = 1.63 and *I*(211)/*I*(112) = 1.94.

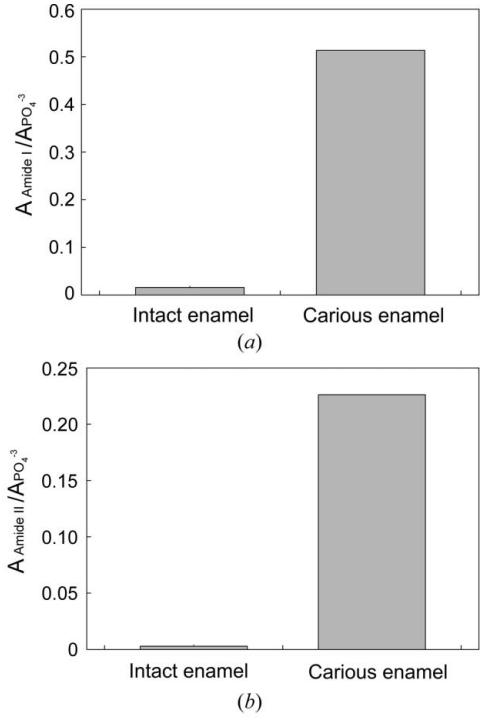

Figure 3
(*a*) Histogram $A_{\text{Amide I}}/A_{PO_4^{3-}}$. (*b*) Histogram $A_{\text{Amide II}}/A_{PO_4^{3-}}$.

Therefore, the texture index can be calculated in the following way,

$$R(300) = I(211)/I(300)/1.63,$$
$$R(112) = I(211)/I(112)/1.94.$$

If $R = 1$, then crystallites of hydroxyapatite are distributed randomly, while $R > 1$ or $R < 1$ indicates a preferable orientation of HAP crystals in the enamel and means formation of texture. Our calculations show that the texture index *R*(300) for intact enamel is equal to 11.3 while for the points (3), (4) and (5) in the fissure canal it is 10.6, 3.16 and 2.35, respectively (see Table 1).

In order to examine the changes in the structure of hard dental tissues during the development of the carious process in the tooth, we can provide semi-quantitative estimations of these changes by analyzing the results of X-ray diffraction presented in Fig. 4 by introducing a crystallinity index proposed by Person *et al.* (1995). According to this method, the crystallinity index for hydroxyapatite crystals can be calculated using the diffraction peaks heights *h*, *a*, *b* and *c* for the peaks (211), (112), (300) and (202), respectively. The main

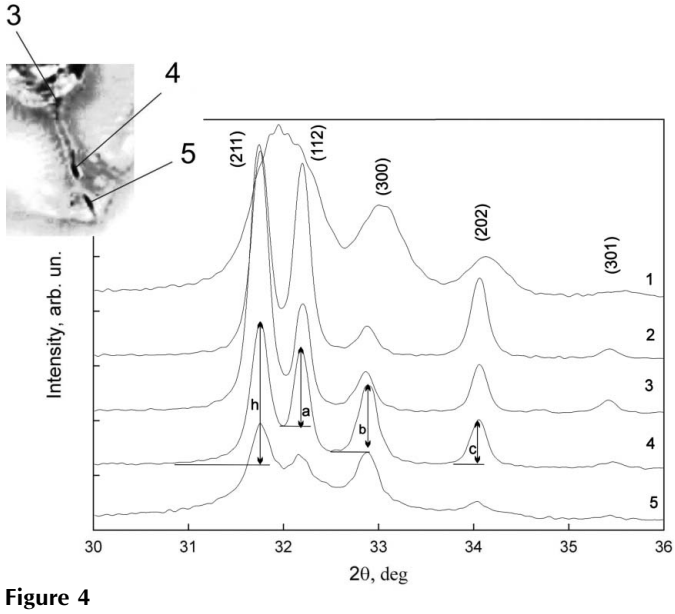

Figure 4
Results of X-ray diffraction. 1, synthesized bio HAP (Goloshchapov *et al.*, 2013). 2, sound enamel (point 1, Fig. 1*a*). 3–5, points 3–5 in the carious canal presented in Fig. 1(*b*) used for the diffraction study.

problem of the proposed technique lies in the correct separation of these peaks in the diffraction pattern. The height of the peak is measured as presented in Fig. 4 for diffraction from the area inside a carious fissure: from the maximum of the diffraction line to the minimum of the line intensity, *i.e.* the hollow formed by two close lines (see Fig. 4). Thus, the crystallinity index, CI, can be determined according to the following expression,

$$\mathrm{CI} = (a + b + c)/h.$$

The calculated crystallinity index for the intact enamel takes the value of 1.11, which coincides with that presented by Xue *et al.* (2008), while for the points (3), (4) and (5) in the carious fissure this index takes values of 0.55, 1.28 and 0.62, respectively (see Table 1).

It is known that the content of the ordered or, in other words, crystalline part of matter in the samples is proportional to the crystallinity index. So a decrease in the index means amorphization of the HAP crystal. The obtained results allow the conclusion to be made that with an increase in the carious cavity size, in our case this is caries of dental enamel fissure, HAP crystals that are ordered in intact enamel along the direction perpendicular to the dentine–enamel junction are randomly distributed with the depth of the carious process in the collagen matrix–protein network. This case corresponds to microcrystalline powder HAP. At the same time, amorphization of hydroxyapatite crystal itself can be observed, which indicates its destruction.

Based on the experimental data, we can determine the size of the hydroxyapatite crystals according to the Scherrer formula,

$$D = K\lambda/(\beta\cos\theta),$$

where D is the size of the crystallites, K is a constant close to 0.9, λ is the wavelength of characteristic radiation for copper, 1.540598 Å, β is the half-width of X-ray line (211) used for the analysis, and θ is the Bragg angle for (211), a crystal plane. The obtained results are presented in Table 1. The HAP crystal size for intact enamel is $\sim$40 nm; note that this size is slightly reduced as we move into the fissure (see Fig. 1).

It should be noted that Xue *et al.* (2008) discussed similar investigations of hard dental tissues by X-ray diffraction; however, the size of HAP crystallites determined by those authors considerably differed from that calculated in our studies. It is probable that, while determining the size of the HAP crystallites in the enamel and dentine, Xue *et al.* (2008) made a mistake. This could be due to a low angle resolution of the plane X-ray detector used for obtaining Debye patterns. Diffraction planes (211) and (112) merged into a common diffraction peak [as can be easily seen from the plots presented in Xue *et al.* (2008)] and the half-width of this peak was used for the calculations of the HAP crystal size.

Using an inverse calculation involving the Scherrer equation for determining the amount of hydroxyapatite crystals and the data of Xue *et al.* (2008) concerning the size of the HAP crystals, we can determine the half-width of the diffraction lines used for the calculation. By comparing the calculated value of the diffraction peak half-width and experimental half-width of an image in the paper by Xue *et al.*, it can be seen that Xue *et al.* erroneously used unresolved diffraction peaks of the (211) and (112) reflections for its calculation whereas the use of diffraction plane (211) was required.

This is why it is so important to apply a high-precision goniometer and detector with a high space resolution when analyzing low-symmetry crystal systems.

More precise analysis of the microstructure and nanostructure of biological composites can be made using small-angle X-ray scattering methods (Gourrier *et al.*, 2007). Such methods offer the advantage of having an almost microscopic spatial resolution, thus yielding an extremely powerful tool for the characterization of nano-sized polymers and composites (Zafeiropoulos *et al.*, 2005).

5. Results

The results presented above clearly demonstrate the difference between intact enamel and enamel under emerging carious fissure. A greater crystal size (40 nm), high texture and crystallinity indices as well as a minimum of organic content all characterizes intact enamel and agree with up-to-date concepts on the structure of enamel and results of works similar to our research (Tiznado-Orozco *et al.*, 2009; Low, 2004; Person *et al.*, 1995; Xue *et al.*, 2008). At the same time, emerging fissure caries is characterized by an increase in organic content in the fissure canal according to IR-spectromicroscopy data. Analysis of different points in the fissure canal by X-ray diffraction showed a decrease in the sizes of HAP crystallites with depth, which could be due to specific features in the dental structure but also may be a result of the carious process connected with diminishing crystallinity and texture indices.

6. Conclusions

Fissure caries of enamel is characterized by an increase in the number of deformation and stretching vibrations of N—C—O, N—H and C═O bonds, a decrease in the crystallinity and texture indices as well as by the absence of the predominant orientation of HAP crystals in the affected enamel, implying a destructive disease in the organic matrix of hard tooth tissues. Owing to subsurface demineralization, dental enamel crystals themselves are further destroyed.

This work was carried out with the support of the Federal Target Program 'Scientific and research pedagogical staff of innovative Russia' for 2009–2013, GK8153, and the Russian Foundation for Basic Research No. 13-02-97500. This work is based in part upon research conducted at the Synchrotron Radiation Center, University of Wisconsin-Madison, which is supported by the National Science Foundation under Award No. DMR-0537588. We acknowledge ANKA synchrotron light source for provision of beam time at the PDIFF beamline.

References

Bykov, V. L. (1998). *Histology, Embryology of Oral Cavity Organs of a Human.* Tutorial. St Petersburg.

Dunlop, J. W. C. & Fratzl, P. (2010). *Annu. Rev. Mater. Res.* **40**, 1–24.

Fried, D., Wheeler, C. R. & Le, C. Q. (2003). *IR Spectromicroscopy of Laser Irradiated Dental Hard Tissues*, http://citeseerx.ist.psu.edu.

Goldberg, M., Septier, D., Lécolle, S., Chardin, H., Quintana, M. A., Acevedo, A. C., Gafni, G., Dillouya, D., Vermelin, L. & Thonemann, B. (1995). *Int. J. Dev. Biol.* **39**, 93–110.

Goloshchapov, D. L., Kashkarov, V. M., Rumyantseva, N. A., Seredin, P. V., Lenshin, A. S., Agapov, B. L. & Domashevskaya, E. P. (2013). *Ceram. Int.* **39**, 4539–4549.

Gourrier, A., Wagermaier, W., Burghammer, M., Lammie, D., Gupta, H. S., Fratzl, P., Riekel, C., Wess, T. J. & Paris, O. (2007). *J. Appl. Cryst.* **40**, s78–s82.

He, L.-H., Carter, E. A. & Swain, M. V. (2007). *Anal. Bioanal. Chem.* **389**, 1185–1192.

Jenkins, G. N. (1978). *The Physiology and Biochemistry of the Mouth*, 4th ed., p. 599. Oxford: Blackwell.

Karlinsey, R. L., Mackey, A. C., Walker, E. R., Frederick, K. E. & Fowler, C. X. (2009). *J. Dent. Oral Hyg.* **1**, 52–58.

Krutchkoff, D. J. & Rowe, N. H. (2009). *J. Dent. Res.* **50**, 1589–1593.

Low, I.-M. (2004). *J. Am. Ceram. Soc.* **87**, 2125–2131.

Maertena, A., Zaslansky, P., Mochales, C., Traykova, T., Mueller, W. D., Fratzl, P. & Fleck, C. (2013). *Dent. Mater.* **29**, 241–251.

Person, A., Bocherens, H., Saliège, J.-F., Zeitoun, V. & Gérard, M. (1995). *J. Archaeol. Sci.* **22**, 211–221.

Rey, C., Combes, C., Drouet, C., Sfihi, H. & Barroug, A. (2007). *Mater. Sci. Eng. C*, **27**, 198–205.

Ślósarczyka, A., Paszkiewicza, Z. & Paluszkiewicz, C. (2005). *J. Mol. Struct.* **744–747**, 657–661.

Tiznado-Orozco, G. E., García-García, R. & Reyes-Gasga, J. (2009). *J. Phys. D*, **42**, 235408.

Xue, J., Zhang, L., Zou, L., Liao, Y., Li, J., Xiao, L. & Li, W. (2008). *J. Synchrotron Rad.* **15**, 235–238.

Yagi, N., Ohta, N., Matsuo, T., Tanaka, T., Terada, Y., Kamasaka, H. & Kometani, T. (2010). *J. Phys. Conf. Ser.* **247**, 012024.

Yamakoshi, Y., Tanabe, T., Oida, S., Hu, C.-C., Simmer, J. P. & Fukae, M. (2001). *Arch. Oral. Biol.* **46**, 1005–1014.

Zafeiropoulos, N. E., Davies, R. J. & Roth, S. V. (2005). *Macromol. Rapid Commun.* **26**, 1547–1551.